Abundance of rare and elusive species: Empirical investigation of closed versus spatially explicit capture-recapture models with lynx as a case study

Laetitia Blanc, Eric Marboutin, Sylvain Gatti, Olivier Gimenez

HAL Id: hal-03499359
https://hal.science/hal-03499359

Submitted on 25 Dec 2021

1 ABUNDANCE OF RARE AND ELUSIVE SPECIES: EMPIRICAL INVESTIGATION OF CLOSED VS.

2 SPATIALLY EXPLICIT CAPTURE-RECAPTURE MODELS WITH LYNX AS A CASE STUDY

3

4 **Laetitia Blanc[1,2], Eric Marboutin[2], Sylvain Gatti[2], and Olivier Gimenez[1]**

5 [1] Centre d'Ecologie Fonctionnelle et Evolutive, UMR 5175, campus CNRS, 1919 Route de

6 Mende - F34293 Montpellier cedex 5

7 [2] Office National de la Chasse et de la Faune Sauvage – CNERA Prédateurs-Animaux

8 déprédateurs, ZI Mayecin - F38610 Gières.

9

10 **ABSTRACT**

11 Effective conservation and management require reliable monitoring methods and estimates of

12 abundance to prioritize human and financial investments. Camera trapping is a non-invasive

13 sampling method allowing the use of capture-recapture (CR) model to estimate abundance

14 while accounting for the difficulty of detecting individuals in the wild. Here, we investigated

15 the relative performance of classical closed CR models and spatially explicit CR models

16 (SECR) that incorporate spatial information in the data. Using simulations, we considered

17 four scenarios comparing low vs. high detection probability and small vs. large populations

18 and confronted abundance estimates obtained from both approaches. Standard and SECR

19 models both provided lowly biased abundance estimates but precision was improved when

20 using SECR models. The associated confidence intervals also provided better coverage than

21 their non-spatial counterpart. SECR models exhibit better statistical performance than

22 standard closed CR models and allow producing sound management strategies through

23 density maps of activity centers. To illustrate the comparison, we considered the Eurasian

24 lynx (*Lynx lynx*) as a case study and provided the first abundance estimates of a local

25 population in France.

26 *Keywords*: abundance, relative bias, camera trapping, capture-recapture models, *Lynx lynx*,

27 root mean square error, simulations, spatially explicit capture-recapture models.

28

29 **INTRODUCTION**

30 The presence of large carnivores - wolves, bears, lynxes, and wolverines - usually results in

31 strong socio-cultural issues in all societies, Europe making no exception. These species share

32 common features such as large territories and the need for a large mosaic of natural habitat

33 and preys, potentially competing with human activities, e.g., hunting and livestock farming.

34 Such conflicts, in combination with habitat loss, have led to local extinction of large

35 carnivores in many areas. While almost extinct at the beginning of the 20th century in many

36 European countries, large carnivores have slowly recovered via reintroduction or natural re-

37 colonization through dispersal.

38 In this context, the Bern convention (1979), the European Habitats Directive (1992) as well as

39 the International Union for Conservation of Nature (IUCN) Red list provided specific indexes

40 and rules to assess the conservation status of species and to help checking how management

41 decisions could meet the conservation requirements. Abundance was defined as one of the

42 key estimates needed in assessing species' status and is the state variable of interest in most

43 ecological research and monitoring programs involving management and conservation of

44 animal populations (Nichols and MacKenzie 2004). Indeed, reliable estimates of population

45 size are essential to evaluate conservation and wildlife management programs such as

46 reintroduction programs. However, large carnivores are difficult to monitor since they are

47   elusive, living at low densities over wide areas and usually solitary and mostly nocturnal.

48   Exhaustive counts are therefore often expensive, time consuming and sometimes impractical.

49   In order to assess population trends in elusive and wide-ranging population, non-invasive

50   survey methods have been increasingly used over the last decade. In particular, camera-

51   trapping methods combined with capture-recapture (CR) modeling have become a standard

52   tool to estimate carnivores' abundance while accounting for detectability less than 1 (e.g.,

53   tigers *Panthera tigris*: Karanth et al. 2006, Karanth and Nichols 1998; ocelots *Felis pardalis*:

54   Trolle and Kéry 2003; snow leopards *Uncia uncia*: Jackson et al. 2006; jaguars *Panthera*

55   *onca*: Silver et al. 2004). Standard CR models usually assume geographical closure (no

56   movement in or off the sampling grid). However, this assumption is often violated, especially

57   for mammals with large home range. Another major assumption of these models is that no

58   individual within the sampled area has a zero probability of being captured. To deal with these

59   issues, an alternative approach known as spatially-explicit CR modeling (SECR) was recently

60   developed (Royle and Young 2008, Borchers and Efford 2008). This method has been applied

61   to a large number of taxa (e.g., birds: Efford 2004, Borchers and Efford 2008, Efford et al.

62   2009a; cetaceans: Marques et al. 2010; stoats: Efford et al. 2009b; bears: Obbard et al. 2010

63   and lizards: Royle and Young 2008). Here, the probability of detection for each trap is

64   modeled as a function of distance between a latent variable, the individual activity center

65   (equivalent to the home range center), from which animals move randomly, and the camera

66   trap where they have been captured. This model does not rely on the assumption of

67   geographic closure by accounting for the fact that animals move and that detection probability

68   depends on their center of activity (Gardner et al. 2009).

69   In this paper, our objectives were twofold. First, we aimed at evaluating the relative

70   performance of SECR methods vs. conventional non-spatial CR models in estimating

71   abundance in the context of carnivore conservation. Most of the studies assessing bias in

72   spatial models compared abundance estimates using real datasets rather than simulated data,

73   hence the impossibility to infer bias and precision (e.g., Gardner et al. 2009). Recent papers

74   dealing with SECR models and simulations (Efford 2004, Royle and Young 2008, Borchers

75   and Efford 2008, Efford 2011) focused on the performance of different methods to estimate

76   density (e.g., nested subgrid vs. inverse prediction, likelihood-based vs. Bayesian methods)

77   but did not formally compare SECR and non-spatial models. Therefore, we carried out a

78   simulation study with several scenarios comparing low vs. high detection probability and

79   small vs. large populations to quantify the performances of parameter estimates using both

80   SECR and non-spatial models. We also suggested how the simulations results could be used

81   to improve the trapping design when necessary. Second, we used the two methods to analyze

82   a real dataset from a camera-trapping experiment with the Eurasian lynx (*Lynx lynx*) in the

83   French Jura Mountains. This population originates from reintroductions in Switzerland in the

84   70's. Although listed as a species of Least Concern given its wide range (IUCN, 2001), habitat

85   loss, prey depletion, and poaching are still regarded as potential threats. Up to now, the main

86   monitoring program for lynx in France was based on indirect signs (i.e., tracks, scat, hair, and

87   other signs) collected by a network of volunteers (state employees, hunters, naturalists,

88   farmers, and mountain guides). While the use of indirect signs is often the most effective and

89   least expensive method for estimating the distribution of carnivores, the resulting estimates of

90   population parameters such as abundance are often approximate. Camera-trapping monitoring

91   has recently been initiated in France in order to monitor lynx population and evaluate the

92   conservation status of a population where problematic interactions between hunters and lynx

93   exist. We provided the first estimate of Lynx abundance for this French population. Finally,

94   recommendations are provided for the conservation of elusive species, with an emphasis on

95   large carnivores and their monitoring.

96   MATERIAL AND METHODS

97   **Simulation study design**

98   We considered that our population was demographically and geographically closed (i.e. no

99   birth, death, immigration or emigration during the sampling period) to apply CR models to

100 estimate abundance. Lynx are long-lived animals (Sunquist and Sunquist 2002) and the

101 camera-trap sampling period was made short enough so that no deaths or births were assumed

102 to occur during this period. In addition, the trapping session was timed outside the dispersal

103 period for subadults.

104 In order to compare the performance of the standard vs. the SECR methods in estimating

105 abundance, we simulated 100 datasets with a particular spatial organization. We considered

106 four scenarios comparing low vs. high detection probability and small vs. large populations.

107 These scenarios were used to evaluate relative bias in parameter estimates, the precision and

108 the coverage of 95% confidence and credible intervals (CI hereafter for Bayesian credible

109 intervals or Frequentist confidence intervals indistinctively). Each dataset was created using

110 the traps configuration from the monitoring of the lynx in the study area (see case study

111 below) but we did not use any constraints to mimic lynx behavior simulating the datasets. The

112 number of capture occasions was set to $k = 15$ and the actual population size to $N = 10$ or $N =$

113 50 depending on the scenario. The simulations were based on the SECR model formulation.

114 We simulated N individual activity centers using their coordinates. Then, we evaluated

115 whether we could *a posteriori* reliably estimate from the model the actual number and

116 location of activity centers we had simulated. We proceeded to the simulation in two steps,

117 first a point process component that describes the spatial distribution of the centers of activity,

118 second an observation process component that makes the connection between the detection of

119 an individual and its center of activity given the spatial distribution of traps.

120   *a) Point process*

121   We assumed a fixed and known number of activity centers s_i (similar to home range centers)

122   with geographic coordinates $s_i = (s_{xi}, s_{yi})$ for each individual i ($i = 1, …, N$) of the population.

123   We assumed that these centers of activity were uniformly distributed over a region S, an

124   arbitrary polygon containing the trapping array.

125     $s_i \sim$ Uniform (S)   (Eq. 1)

126   In order to simulate capture histories we assumed that the probability of each individual to be

127   captured was a function of the distance between its activity center and the trap.

128   *b) Exposure to traps*

129   The detection probability of an individual at a given trap was a decreasing function of the

130   distance from the activity center to that trap: the further the activity center was from the trap,

131   the less likely the animal was exposed to capture. Thus, we first defined a distance matrix $D_{i,j}$

132   as the Euclidean distance between every activity centers i and trap j:

133     $D_{i,j} = \sqrt{\left(s_{xi} - x_j\right)^2 + \left(s_{yi} - y_j\right)^2}$ (Eq. 2)

134   Second, we modeled the exposure of each individual as a function of distance and two other

135   parameters:

136     $E0_{i,j} = \lambda_0 \exp\left(-D_{i,j}^2 / \sigma\right)$ (Eq. 3)

137   where λ_0 is the baseline encounter rate, i.e. the expected number of captures of individual i at

138   trap j during a sampling occasion when an individual's activity center s_i is located precisely at

139   trap j, and parameter σ (in km) controls the shape of the distance function, reflecting how fast

140   the exposure decreases with distance. The greater σ is, the faster the exposure decreases with

141   distance.

142   *c) Capture process*

143   If an individual *i* is exposed to trap *j*, we assumed a capture probability $p_{i,j}$. The distance

144   function allows the development of the capture process model. The increase of the exposure

145   to traps translates into an increase of the capture probability and was modeled with an

146   exponential function:

147    $$p_{i,j} = 1 - \exp\left(-E0_{i,j}\right)$$ (Eq. 4)

148   We assigned two different values for λ_0 (0.03 and 2) and one value to σ (1.5) depending on the

149   scenario. All combinations of all levels of N, λ_0 and σ were tested resulting in 4 scenarios. For

150   each scenario and each simulated dataset, we constructed the distance matrix $D_{i,j}$ between the

151   simulated activity centers and the traps location. The distance matrix was used to estimate for

152   each individual a per trap capture probability $p_{i,j}$. Then, we performed a binomial trial with

153   parameters N and $p_{i,j}$ to determine whether the individual was captured or not. Since detection

154   is not perfect, only *n* out of the N total individuals from the population were detected. We

155   compiled for each of the J traps the number of occasions K an individual *i* was detected. Thus,

156   for each trap and each individual, a code number ranging from 0 to K indicated how many

157   occasions each individual was captured. These count histories were used to fit SECR models.

158   Finally, we analyzed the capture histories of the *n* individuals under the standard and SECR

159   models.

160   **Model formulation**

161   *a) Standard CR models*

162   We first calculated abundance estimates by accounting for detection probabilities using

163   standard CR models. We considered different sources of variation in capture probabilities. In

164   addition to a model with no variation in the detection probability (model M_0), we considered

165   behavioral responses to trapping (model M_b), differences in capture probabilities over time

166   (model M_t), while the most complex models included among-individual heterogeneity in

167   capture probabilities (model M_h) (Otis et al. 1978, Williams et al. 2002). In addition, we

168   considered four models that were combinations of these sources of variation (Models M_{bh},

169   M_{th}, M_{tb}, and M_{tbh}). For each simulated dataset, the Akaike's Information Criterion (AIC) was

170   used to select the model that best described our dataset (Burnham and Anderson 2002). These

171   analyses were achieved via maximum likelihood with the R package Rcapture (Baillargeon

172   and Rivest 2007).

173   *b) SECR model implementation using a Bayesian approach*

174   Each camera trap reflected the location of capture, which, in turn, provided insight into the

175   activity centers coordinates of each lynx. The SECR model has the advantage to incorporate

176   spatial heterogeneity while estimating abundance (Royle et al. 2009a, Royle et al. 2011, Royle

177   et al. 2009b). More specifically, the SECR model makes explicit the distinction between a) a

178   latent component for the spatial point process of the (unknown) location of the activity centers

179   (Eq. 1) and b) an observation component that describes how the observed data arise from the

180   point process (Eq. 4).

181   We adopted a Bayesian approach (McCarthy 2007) to fit the SECR model. It made the

182   analysis convenient as the activity centers are treated as random effects that are relatively easy

183   to deal with in the Bayesian framework (King et al. 2009). The Bayesian approach combines

184   the likelihood with prior probability distributions of the parameters to obtain the posterior

185   distribution of the parameters of interest based on Bayes' theorem. We used Markov Chain

186   Monte Carlo (MCMC) methods to simulate observations from the posterior distributions.

187   Regarding priors for parameters, we considered that we did not have any information about

188   the spatial distribution of the activity centers of the simulated individuals thus we assumed

189   they were uniformly distributed over S. We chose a Uniform(0,15) distribution for σ and we

190   assigned a Gamma(0.1,0.1) distribution to λ_0.

191   To obtain an estimate of abundance, we used a data augmentation approach (Royle and Young

192   2008). We augmented the data set with 100 individuals and we associated to every individual

193   a latent indicator z_i. The encounter histories of the 100 individuals initially contained only

194   zeroes. Some of these individuals were not captured during the intensive camera trapping but

195   belonged to the population. The z_i indicator reflects the probability ψ of an individual to be a

196   member of the population. We assumed a Uniform(0,1) prior for ψ that we added as an

197   additional layer to our model. We defined z_i as a binary variable equals to 0 when the

198   individual *i* is not a member of the population and 1 otherwise.

199   The abundance N was obtained as a derived parameter by adding all the presence indicators

200   z_i. These analyses were implemented in WinBUGS (Spieghalter et al. 2003) called from R

201   using package R2WinBUGS (Sturtz et al. 2005).

202   *c) Evaluating the performance of the two methods*

203   We evaluated the performance of the standard CR models and the SECR models by

204   comparing the abundance estimates of the two methods used on each 100 datasets simulated

205   to the true value of abundance. As a result, we were able to quantify the potential bias in

206   parameter estimates obtained for both models. We looked at the relative bias in $\hat{N}$, the

207   estimator of N, calculated as (E[$\hat{N}$] − N) / N which can be approximated as the average over

208   the 100 iterations of the difference between the estimated abundance under the model

209   considered and the true parameter value $\sum_{i=1}^{100} \hat{N}_i / 100 - N$. To assess the precision, we

210   calculated the Root Mean Square Error (RMSE) as $\sqrt{E((\lceil \hat{N} \rceil - N)^2)} \approx \sqrt{\sum_{i=1}^{100} (\hat{N}_i - N)^2 / 100}$.

211   A low RMSE is characteristic of a good trade-off between low bias and high variance. Finally,

212   we looked at the 95% confidence interval coverage by determining and averaging over all

213   simulations whether the interval contained the true value.

214   **Eurasian lynx in French Jura Mountains**

215   Lynx is a solitary nocturnal species, living in forested areas. It can be individually identified

216   based on the photographs of their unique pelage patterns (e.g., Zimmermann and

217   Breitenmoser 2007). Our study area was located in the French department of Jura. A 480 km²

218   zone was considered in the southern center of the Jura department between the Vouglans lake

219   and the southern border of Doubs department. This study area was delimited using knowledge

220   on lynx habitat and forest continuity. In order to maximize detectability, several steps were

221   followed: 1) Camera traps were set at optimal locations (on game path, hiking trail, forest

222   road) based on previous signs of lynx presence and on local knowledge; 2) In theory, all

223   individuals should have a non-null detection probability to use standard capture-recapture

224   models (Karanth and Nichols 1998). It is not necessary for SECR models (Royle et al. 2009a).

225   Thus, the study area was divided into a grid of 2.7 km × 2.7 km cells (Zimmermann et al.

226   2007) where one of two cells was sampled, leading to 33 cells sampled from February to

227   April 2011. This grid size and sampling design ensure that at least one camera trap site is set

228   in each potential lynx home range; 3) At each trapping site, two camera traps with infrared

229   trigger mechanism were set in order to photograph both flanks of the animal allowing a high

230   level of confidence in individual identification. Date, time and location of each photographic

231   capture of a lynx were recorded; 4) Camera traps were checked weekly to change memory

232   cards and batteries. The sampling period was divided into 15 occasions, one occasion being

233   defined as 4 successive trap nights. The results of the SECR model were used to build a

234   density map of the lynx activity centers. For each of the MCMC iterations, we plotted the

235   centers of activity of the individuals belonging to the population ($z_i = 1$) on successive layers.

236   For every layer, we divided the region S into squares of 500×500 m then we calculated the

237   mean number of activity centers falling into each square. R and WinBUGS codes are

238   available on request from the first author.

239   **RESULTS**

240   **Simulation study to compare spatial vs. non-spatial models**

241   For each scenario and each simulated dataset, we reported the abundance posterior median

242   estimate and its 95% credible interval for the SECR model and the abundance point estimate

243   with its 95% confidence interval from the non-spatial model (Fig. 1). Scenario A represented a

244   small population with a low detection probability mimicking the Eurasian lynx dataset. Both

245   models similarly slightly overestimated abundance: the non-spatial model displayed a relative

246   bias of 0.096 and the SECR model relative bias was 0.121. Scenario B represented a large

247   population with a low detection probability. The non-spatial model clearly underestimated the

248   population size with a relative bias of −0.08 while the SECR model slightly underestimated it

249   with a −0.016 relative bias. Scenario C corresponded to a small population with a high

250   detection probability. For most datasets, the non-spatial model provided estimates close to the

251   actual abundance (relative bias around 0.007) but with large confidence intervals and the

252   SECR model also provided unbiased estimates (relative bias around −0.02) and small credible

253   intervals. Finally, scenario D represented an ideal situation with a large population and a high

254   detection probability. The non-spatial model slightly overestimated abundance (relative bias =

255   0.026) while the SECR model provided values close to the actual abundance (relative bias =

256   0.0002). RMSE clearly revealed that the SECR model provided a better balance between bias

257   and variance for all scenarios than the non-spatial model. With regard to CI coverage, the

258   confidence interval of the non-spatial model included the true abundance value in only 73 to

259   78 out of the 100 simulated datasets depending on the scenario. The credible interval of the

260   SECR model included the true value in 92 to 99 datasets (Table 1). Credible intervals of the

261   SECR model provided better coverage than confidence intervals as provided by standard

262   closed CR models.

263   **Lynx case study**

264   Data were collected between February and April 2011 from 33 trap sites resulting in 1980 trap

265   nights. One site was found effective during less than 50% of the trapping nights. It was

266   removed from the analysis reducing the theoretical effort to 1816 effective trapping nights.

267   The study provided an encounter history for 9 individuals that were photographed on 14 of

268   the 32 trap sites. Individuals were captured on up to six different sites and the maximum

269   distance moved by one individual between captures was 27.6 km. Model selection ranked M_h

270   incorporating individual heterogeneity in capture probability as the best model followed by

271   M_0 assuming constant capture probability. Average estimated detection (over individuals) was

272   0.14 and the estimated abundance using M_h was 12 individuals (95% CI 7.14−20.27). For the

273   SECR model, the baseline encounter rate at a given camera (λ_0) was 0.05 photographs

274   occasion^{-1} (95% CI 0.03−0.15) while the movement parameter σ was estimated to 1.45 (95%

275   CI 0.16−0.58). The abundance was estimated to 12.04 individuals (95% CI 9.0−18.0).

276   Posterior estimates of activity centers' locations of the 9 individuals photographed are shown

277   in Fig. 2. There was a lot of spatial variation in the location of estimated activity centers, most

278   of them being concentrated in the center and in both south-eastern and western corners of the

279   trap array.

280   **DISCUSSION**

281   Information on wildlife population responses and dynamics are essential complements to the

282   human dimensions, habitat, and ecosystem functioning that go into conservation planning and

283   monitoring (Mills 2007). Using the Eurasian lynx as a case study, we demonstrated how

284   cutting-edge analytical methods could be used to estimate and infer abundance of a rare and

285   elusive species using sound monitoring protocols. This is a crucial step when implementing

286   any conservation strategy so as to be able e.g. to characterize the population status before any

287   action is undertaken, and re-evaluate it once management has been engaged.

288   **Comparison of abundance estimates from spatial vs. non-spatial models**

289   Albeit the difference in the relative bias between the non-spatial and the SECR model is

290   trivial, the RMSE and the CI coverage both support the conclusion that the SECR model

291   provides better estimates of abundance. Indeed, our simulations have highlighted that for

292   scenario A, mimicking the lynx dataset, and scenario C, abundance estimates should be used

293   with caution since the spatial model tended to overestimate the actual abundance while the

294   non-spatial model appeared to be closer to the real abundance value. The positive relative bias

295   may be caused by the proportion of individuals that move out or partially out of the trapping

296   array creating an inflated estimate of abundance. Nevertheless, confidence and credible

297   interval coverage and RMSE revealed that the SECR model performed best whatever the

298   scenario we considered. For the other scenarios, B and D - representing a large population

299   with respectively a low and high detection probability - abundance estimates were closer to

300   the actual value when using the spatial model. The three deviation indices (relative bias,

301   RMSE and interval coverage) supported this conclusion.

302   Spatially-explicit CR modeling is an emerging analytical tool that has mainly been used to

303   estimate densities because it does not rely on the assumption of geographic closure (Efford

304   2004). Obbard et al. (2010) and Gray and Prum (2012) evaluated the performance of the

305   SECR models while estimating density by comparing density estimates using SECR with

306   those obtained from conventional approach in which the effective survey area is estimated

307   using a boundary strip width. SECR models were recommended in both studies but they could

308   not infer bias since the actual density was unknown. Efford (2004) and Borchers and Efford

309   (2008) assessed the performance of SECR by simulating data from a regular grid of trap.

310   They used alternative methods for fitting the spatial detection model, that is inverse prediction

311   and maximum likelihood while the current study used data augmentation and MCMC (Royle

312   and Young 2008; Royle et al. 2009a, b). Regardless of the method, the importance of spatial

313   nature of the sampling process in capture probability modeling is clearly supported by our

314   findings. Modeling the capture probability also avoids substantial bias in estimating

315   abundance. By making capture probability a function of both the location of the activity

316   centers and their distance from the camera traps, SECR models allow efficient use of spatial

317   information contained in CR data.

318   We acknowledge that we could not cover all possible scenarios in our simulations. In

319   particular, our results were obtained for scenarios that did not account for specificities of the

320   species biology, such as sex-related differences in home range size for instance (Sollmann et

321   al. 2011). Furthermore, we did not take into account the importance of traps configuration that

322   can have large effects on the number of individuals detected. In our study, the traps were

323   placed mainly on trails because lynx use the easiest way to go from one location to another.

324   Further work is needed to determine the optimal number and location of traps in order to

325   minimize the human and financial costs of fieldwork while maximizing the precision of

326   abundance estimates. Simulation studies like the one we have conducted here may help in that

327   purpose. SECR models allow the incorporation of variables affecting detection probability

328   hence providing managers the opportunity to modify cameras distribution to improve capture

329   success (Royle et al. 2011).

330   Non-invasive sampling methods such as camera trapping or molecular tracking are commonly

331   used to monitor elusive and wide-ranging populations of large carnivores, as neither of them

332   requires physical captures. These methods can provide estimates of population parameters,

333   like population size, dispersal distance, population growth rate (Marescot et al. 2011), survival

334   (Cubaynes et al. 2010), recruitment and immigration rate (Karanth et al. 2006). They seemed

335   particularly relevant for the Eurasian lynx whose individual coat patterns allow the

336   identification on photographs that could be used with capture-recapture models to estimate

337   abundance and density. Furthermore, the advantage of camera-trapping for estimating

338   abundance is that it requires only a single sampling session, in other words repeated sampling

339   is not required (Efford et al. 2009). However, this technique requires reliable photographs

340   from which individuals can be univocally identified, otherwise risking bias in population size

341   estimates (overestimation if two photographs belonging to the same individual are considered

342   as two different individuals, underestimation if two photographs of different individuals are

343   wrongly considered as a single individual). The issue of misidentification error has recently

344   received interest (Yoshizaki et al. 2009; Morrison et al. 2011).

345   **Management implications**

346   With rare and elusive species, we recommend caution when using standard or even spatially-

347   explicit capture-recapture models since commonly few data are available. Even though

348   previous studies have demonstrated the utility of non-invasive sampling methods (e.g., Petit

349   and Valière 2006) and the analysis of data collected through CR techniques (e.g., Rees et al.

350   2011) when few data are available, the confidence and credible intervals still remain large. A

351   preliminary simulation study is useful to determine which factors affect abundance estimates

352   (number of camera traps and their location in particular). To help in this objective, we provide

353   R code to reproduce our simulation exercise and adapt it for one's own purpose (See

354   Supplementary Information). Pending these precautions, spatially explicit CR models provide

355   useful information that can be used to produce sound management strategies for carnivores. In

356   particular, the density map of the posterior locations of activity centers could be confronted to

357   livestock attacks distribution maps to determine whether correlations exist between hotspots

358   of attacks on livestock and pools of lynx centers of activity. This might help to predict

359   potential conflicts between human activities and predators.

360   **ACKNOWLEDGMENTS**

366   **LITERATURE CITED**

367   Baillargeon, S., and L. P. Rivest. 2007. Rcapture: Loglinear models for capture-recapture in R.

368   Journal of Statistical Software.

369   Borchers, D. L. and M. G. Efford. 2008. Spatially explicit maximum likelihood methods for

370   capture-recapture studies. Biometrics 64:377−385.

371 Burnham, K. P., and D. R. Anderson. 2002. Model selection and inference: a practical

372   information theoretic approach. Second edition. Springer-Verlag, New York, New York,

373   USA.

374 Cubaynes, S., R. Pradel, R. Choquet, C. Duchamp, J. M. Gaillard, J. D. Lebreton, E. Marboutin,

375   C. Miquel, A. M. Reboulet, C. Poillot, P. Taberlet, and O.Gimenez. 2010. Importance of

376   accounting for detection heterogeneity when estimating abundance: the case of French

377   wolves. Conservation Biology 24:621−626.

378 Efford, M. G. 2004. Density estimation in live-trapping studies. Oikos 106:598−610.

379 Efford, M. G. K., D. Dawson, and D. L. Borchers. 2009a. Population density estimated from

380   locations of individuals on a passive detector array. Ecology 90:2676−2682.

381 Efford, M. G., D. L. Borchers, and A. E. Byrom. 2009b. Density estimation by spatially

382   explicit capture-recapture: likelihood-based methods. Pages 255-269 *in* D. L.

383 Efford, M. G. 2011. Estimation of population density by spatially explicit capture–recapture analysis

384   of data from area searches. Ecology 92:2202−2207.

385   Thompson, E. G. Cooch, M. J. Conroy, editors. Modeling demographic processes in marked

386   populations. Springer, New York.

387 Gardner, B., J. A. Royle, and M. T. Wegan. 2009. Hierarchical models for estimating density

388   from DNA mark-recapture studies. Ecology 90:1106−1115.

389 Gray, T. N. E. and S. Prum. 2012. Leopard density in post-conflict landscape, Cambodia:

390   Evidence from spatially explicit capture-recapture. Journal of Wildlife Management

391   76:163−169.

392 Jackson, R. M., J. D. Roe, R. Wangchuk, and D. O. Hunter. 2006. Estimating snow leopard

393   population abundance using photography and capture–recapture techniques. Wildlife Society

394   Bulletin 34:772–781.

395 Karanth, K. U., J. D. Nichols, N. S. Kumar, and J. E. Hines. 2006. Assessing tiger population

396   dynamics using photographic capture-recapture sampling. Ecology 87:2925–2937.

397 Karanth, K. U., and J. D. Nichols. 1998. Estimation of tiger densities in India using

398   photographic captures and recaptures. Ecology 79:2852–2862.

399 King, R., B. J. T. Morgan, O. Gimenez, and S. P. Brooks. 2009. Bayesian analysis of population

400   ecology. CRC Press.

401 Knapp, S. M., B. Craig, and L. P. Waits. 2009. Incorporating genotyping error into non-

402   invasive DNA-based mark–recapture population estimates. Journal of Wildlife Management

403   73:598-604.

404 Marescot, L., R. Pradel, C. Duchamp, S. Cubaynes, E. Marboutin, R. Choquet, C. Miquel, and

405   O. Gimenez. 2011. Capture-Recapture population growth rate as a robust tool against

406   detection heterogeneity for population management. Ecological Applications 21:2898–2907.

407 Marques, T. A., L. thomas, S. W. Martin, D. K. Mellinger, S. Jarvis, R. P. Morrissey, C.

408   Ciminello, and N. DiMarzio. 2010. Spatially explicit capture recapture methods to estimate

409   minke whale abundance from data collected at bottom mounted hydrophones. Journal of

410   Ornithology in press.

411 McCarthy, M. A. 2007. Bayesian methods for ecology. Cambridge University Press,

412   Cambridge, UK.

413 Mills, L. S. 2007. Conservation of Wildlife Populations: Demography, Genetics, and

414   Management. Blackwell Publishing, Malden, Massachusetts, USA.

415 Morrison, T. A., J. Yoshizaki, J. D. Nichols, and D. T. Bolger. 2011. Estimating survival in

416   photographic capture-recapture studies: overcoming misidentification error. Methods in

417   Ecology and Evolution 2:454−463.

418 Nichols, J. D. and J. D. MacKenzie. 2004. Abundance and conservation biology. Animal

419   biodiversity and conservation 27.1:437−439.

420   Obbard, M. E., E. J. Howe, and C. J. Kyle. 2010. Empirical comparison of density estimators

421   for large carnivores. Journal of Applied Ecology 47:76−84.

422   Otis, D. L., K. P. Burnham, G. C. White, and D. R. Anderson. 1978. Statistical inference from

423   capture data on closed animal populations. Wildlife Monograph 62:1–135.

424   Petit, E., and N. Valiere. 2006. Contributed Papers: Estimating population size with

425   noninvasive Capture-Mark-Recapture data. Conservation Biology 20:1062–1073.

426   Rees, S. G., A. E. Goodenough, A. G. Hart, and R. Stafford. 2011. Testing the effectiveness of

427   capture mark recapture population estimation techniques using a computer simulation with

428   known population size. Ecological Modelling 222:3291–3294.

429   Royle, J. A. and K. V. Young 2008. A hierarchical model for spatial capture recapture data.

430   Ecology 89:2281–2289.

431   Royle, J.A., K. U. Karanth, A.M. Gopalaswamy, and N.S. Kumar. 2009. Bayesian inference in

432   camera trapping studies for a class of spatial capture-recapture models. Ecology 90:3233–

433   3244.

434   Royle, J. A., J. D. Nichols, K. U. Karanth, and A. M. Gopalaswamy. 2009. A hierarchical

435   model for estimating density in camera-trap studies. Journal of Applied Ecology 46:118–127.

436   Royle, J. A., A. J. Magoun, B. Gardner, P. Valkenburg, and R. E. Lowell. 2011. Density

437   estimation in a wolverine population using spatial capture-recapture models. The Journal of

438   Wildlife Management 75:604–611.

439   Silver, S. C., L. E. T. Ostro, L. K. Marsh, L. Maffei, A. J. Noss, M. J. Kelly, R. B. Wallace, H.

440   Gómez, and G. Ayala. 2004. The use of camera traps for estimating jaguar Panthera onca

441   abundance and density using capture/recapture analysis. Oryx 38:148–154.

442   Sollmann, R., M. M. Furtado, B. Gardner, H. Hofer, A. T.A. Jácomo, N. M. Tôrres, and L.

443   Silveira. 2011. Improving density estimates for elusive carnivores: Accounting for sex-

444   specific detection and movements using spatial capture–recapture models for jaguars in

445   central Brazil. Biological Conservation 144:1017–1024.

446 Spieghalter, D. J., A. Thomas, and N. Best. 2003. WinBUGS, Version 1.4, User Manual.

447 Sturtz, S., U. Ligges, and A. Gelman. 2005. R2WinBUGS: A Package for Running WinBUGS

448   from R. Journal of Statistical Software 12:1–16.

449 Sunquist, M., and F. Sunquist. 2002. Wild Cats of the World. University of Chicago Press,

450   Chicago, USA.

451 Trolle, M., and M. Kéry. 2003. Estimation of ocelot density in the Pantanal using Capture–

452   Recapture analysis of camera-trapping data. Journal of Mammalogy 84:607–614.

453 Williams, B. K., J. D. Nichols, and M. J. Conroy. 2002. Analysis and management of animal

454   populations : modeling, estimation, and decision making. Academic Press, San Diego,

455   California, USA.

456 Yoshizaki, J., K. H. Pollock, C. Brownie, and R. A. Webster. 2009. Modeling misidentification

457   errors in capture-recapture studies using photographic identification of evolving marks.

458   Ecology 1:3–9.

459 Zimmermann, F., and U. Breitenmoser. 2007. Potential distribution and population size of the

460   Eurasian lynx Lynx lynx in the jura Mountains and possible corridors to adjacent ranges.

461   Wildlife Biology 13:406–416.

462

463 **CAPTIONS**

464

465 Table 1. Summary of the statistical performance of the non-spatial and SECR models. The

466   RMSE is the Root Mean Square Error and CI is either the 95% confidence (non-spatial
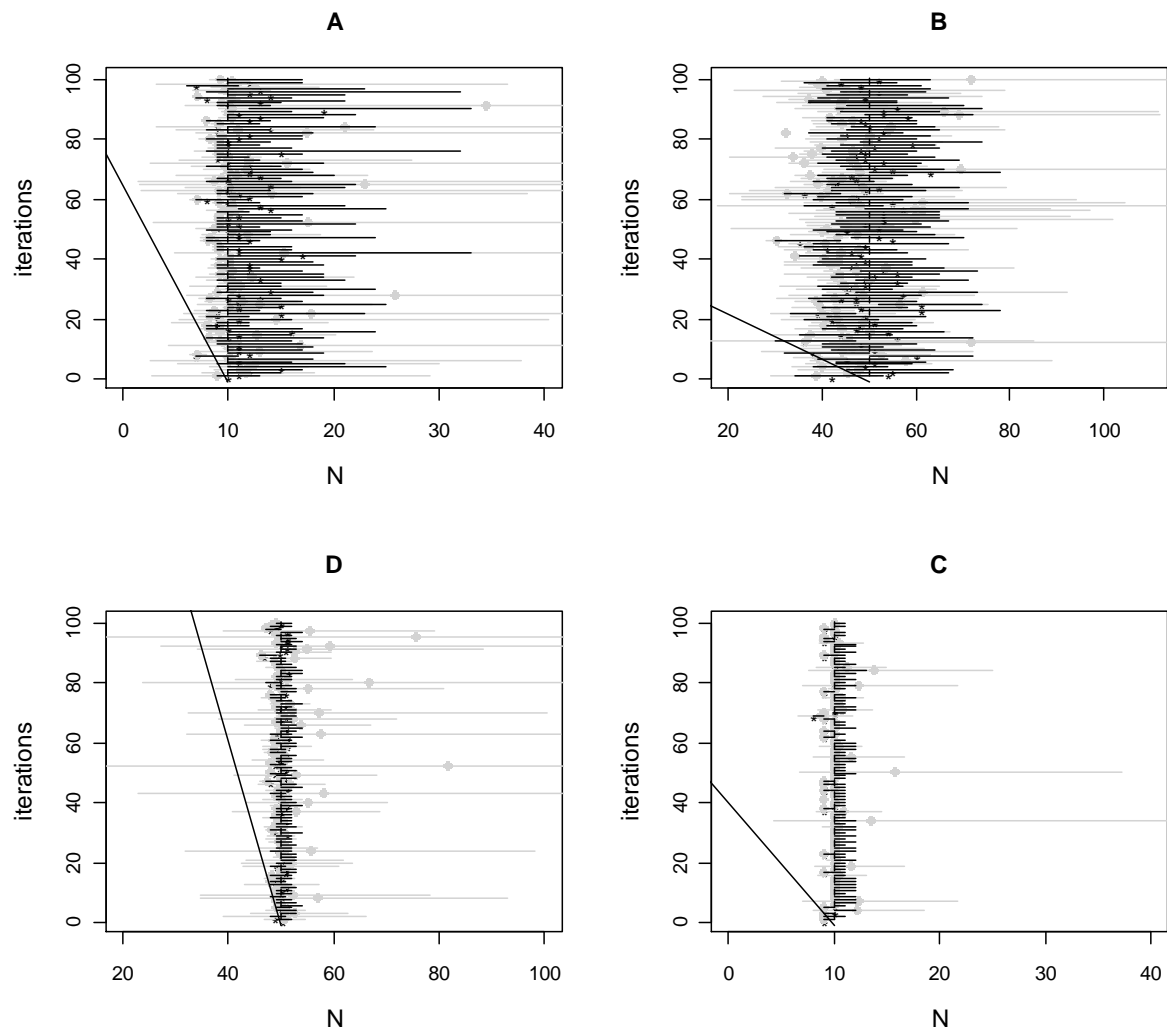
467   model) or the 95% credible (SECR model) interval.

	Scenario	Relative bias	RMSE	CI coverage
Non-spatial model	A	0,10	4,00	75%
	B	-0,08	9,38	76%
	C	0,01	1,03	78%
	D	0,03	5,08	73%
SECR model	A	0,12	2,39	97%
	B	-0,02	5,49	92%
	C	-0,02	0,47	99%
	D	0,00	0,89	96%

468

469

470 Fig. 1. Comparison between abundance estimates obtained from non-spatial models vs. SECR

471 models according to four scenarios (low detection probability (A,B) vs. high detection

472 probability (C, D) and small population size (A,C) vs. large population size (B, D)). With grey

473 dots and lines we displayed respectively estimates and confidence intervals for the non-spatial

474 model. With black asterisk and black lines we displayed posterior means and 95% credible

475 intervals obtained with the SECR model. The vertical dashed line indicates the actual value of

476 abundance.

477 Fig. 2. Map of posterior density of lynx activity centers in French Jura department.

478 Specifically, the map shows $E[N(i) \mid data]$, where $N(i)$ is the number of activity centers

479 located in pixel i. Colors code for the estimated number of activity centers in each $500 \times$

480 500m pixel; triangles indicate mean activity center location for identified individuals; dots

481 indicate camera trap locations; black ones indicate locations where lynx were photographed

482 and grey ones where no lynx was captured.

483

484 Fig. 1

485

486

487

488   Fig. 2

489

490

491